

IMPLEMENTATION STUDY OF A PASSIVE SAFETY FEATURE IN THE RESCUE SYSTEMS OF SMALL AIRCRAFTS

Tomáš HÁJEK  , Robert GRIM , Robert POPELA 


Institute of Aerospace Engineering, Faculty of Mechanical Engineering, Brno University of Technology, Brno, Czech Republic

Article History:

received 14 December 2022
accepted 13 March 2023

Abstract. The aim of this paper is to evaluate the feasibility of implementation of a passive safety feature in the form of an under-fuselage airbag in the rescue systems of small aircraft. The paper presents a multidisciplinary approach for the viability of the implementation. It presents the development of mathematical model for airbag performance analysis. The model is validated against the experimental data to account for various simplifications. Validated mathematical model is used to design a full-scale airbag for the chosen airplane to perform in the designed range. Weight penalty for increased safety is determined.

Keywords: parachute rescue, passive safety, airbag, impact attenuation, experimental validation, ultralight aircraft.

 Corresponding author. E-mail: hajek.t@fme.vutbr.cz

Introduction

Since the first manned flight by the Montgolfier brothers, aviation has become an increasingly important part of everyday life. Unfortunately, as the number of flying vehicles grew, so did the number of accidents. A considerable amount of knowledge has been accumulated through the conscious work of engineers over the past 70 years. This knowledge helped to reduce accident rates and accident severity. According to the report (National Transportation Safety Board, 2011), the rate has steadily decreased over the past 10 years. Unfortunately, the severity of the accidents remains at the same level.

This study was developed as part of a long-term collaboration between the Institute of Aerospace Engineering at Brno University of Technology and the company Galaxy GRS to develop new rescue parachutes for general aviation aircraft, ultimately aimed at reducing the severity of accidents to lower levels.

A PRS is one of the means to reduce the severity of an emergency situation. After activation of the rescue system, a tow rocket is ignited, and the parachute is pulled out of the aircraft. After the lines are tensioned, the parachute is pulled from its pack, initial inflation of the parachute and deceleration begins. To slow the plane down, the parachute must be inflated to increase its area and use its shape to slow down the descent. The area of the parachute is proportional to the weight of the aircraft and the rate of descent required. The area of the parachute is one of the main parameters affecting the minimum deploy-

ment altitude of the rescue system. The larger the area of a parachute, the larger the volume of an inflated parachute, the more air is needed to inflate the parachute, the longer it takes and the higher the minimum deployment altitude. This relationship is shown by (Knacke, 1992) by empirical formula:

$$t_f = \frac{nD_0}{v}. \quad (1)$$

As can be seen in Figure 1a, which was created using data provided by recovery system manufacturers and reported by Šorf (2015), almost 71% of rescue system activations occur below 150 m AGL. Figure 1b shows the limitations of parachute recovery systems in relation to the aircraft's maximum takeoff weight (m_{TOW}) and the minimum altitude for activation of the parachute recovery system. It can be seen that for aircraft heavier than 600 kg the minimum altitude is 110 m AGL. Although the overlap between the incident activation level in Figure 1a and the minimum PRS activation level in Figure 1b is not complete, their meaning is clear.

The aim of this paper is to evaluate the feasibility of implementing a passive safety feature in the form of an under-fuselage airbag in the rescue systems of small aircraft. Such a device has the potential to extend the envelope of a rescue system in terms of minimum activation altitude by absorbing the energy of a higher impact velocity. Therefore, reduce the severity of injuries in emergency landings where the decision to deploy a parachute rescue system is made below a minimum altitude.

Airbags and airbag systems are well known and widely used in various applications such as in automotive, aerospace, or personal safety equipment. The first use of airbags in aviation can be dated to the late 1950s for landing spacecraft for the Mercury project discussed by Norman and Kiker (1967). Followed by extraterrestrial landings of the Luna 9 and 13 reported by Astronautix (2023), Mars Pathfinder and Mars Exploration Rover Missions discussed in Stein et al. (2003), which also used airbags to absorb impact energy. The Orion Crew Exploration vehicle is the more recent example of the use of airbags to cushion the landing of manned spacecraft reported by Tutt et al. (2009). Early theoretical approaches to the airbag attenuation problem were developed by Browning (1963) for cushioning the landing impact for cargo delivery. Building on theoretical foundations, Lee et al. (1991) managed to develop an active gas injection airbag that works similar to the paper crusher, a near-ideal impact energy absorber. Both spacecraft and cargo airbags operate at different ranges or impact speeds and allowable accelerations compared to the scenario studied in this paper.

Both the aviation and automotive industries used internal airbags deployed on impact to protect crew. Airbags are used as impact absorbers, as shown in Figure 2b, as flailing protection of crew, or as pre-tensioners of restraining system which is discussed in full by Hurley (2002). In the past, airbags for flight crew rescue purposes have also been used in out-of-cabin configurations. The first example is the F-111 aircraft escape cabin shown in Figure 2a. The rescue system cushioned the impact of the entire 1230 kg ejection capsule with a sink rate of 8.5 ms^{-1} . The most recent use of external airbags for crew protection comes from Rafael's REAPS, discussed in full (Defense Update, 2005), the helicopter emergency landing cushioning device. Unfortunately, system performance data is not available at this time. Also, unmanned aviation does not use the airbags for safety reasons, but rather as part of the nominal landing sequence. Whether the airbag is combined with a parachute as shown by Manta Air (2023) or is a only cushioning feature of the vehicle as shown by Elbit Systems (2023).

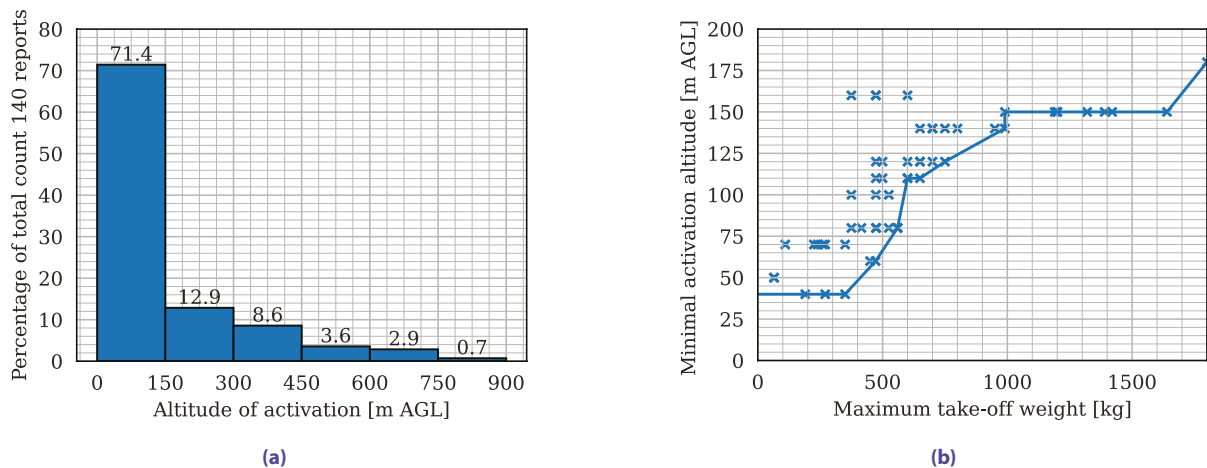
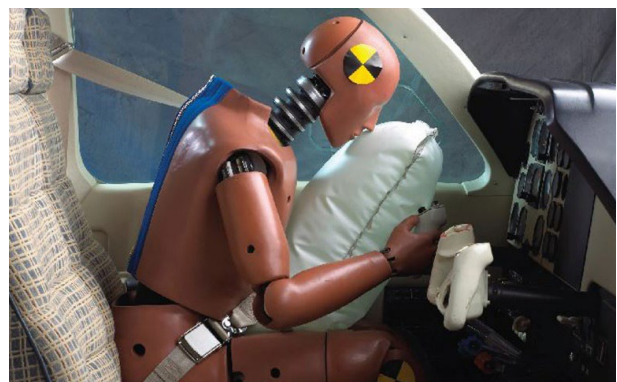


Figure 1. Altitude of parachute recovery. (a) – activation of parachute rescue systems above ground in years 2004–2015; (b) – altitude limits of parachute rescue systems



(a)



(b)

Figure 2. Airbags used for crew protection. (a) – rescue system of the F-111 after airbag activation (Botton, 2021); (b) – AmSafe's Seatbelt Airbag System (SOARS) (Londonson, 2017)

However, from this brief literature review, it can be seen that external airbags were never used to cushion the impact of the manned fixed-wing aircraft under the rescue parachute. Such an approach is unprecedented in passenger aviation. For the feasibility assessment of a novel approach to crew safety in small aircraft, two main research questions need to be answered. First, is it possible to design an under-fuselage airbag with such a performance that would allow a lower minimum height for parachute rescue system activation? Second, what's the weight trade-off with the increased security?

1. Methodology

To answer the raised questions, a mathematical model was built. The results were first validated with previously published cases. In the next step the small experimental airbag model was built to validate the performance of the airbag and the mathematical model under conditions of an emergency landing.

The validated mathematical model was then used to design the full-scale airbag for the chosen airplane. When the performance parameters of the full-scale airbag were known, the weight of the airbags and components needed for its operation could have been determined.

1.1. Mathematical model of airbag attenuation problem

The mathematical model evaluating the performance of a single airbag, decelerating a mass fixed on top, with a venting mechanism was built. The model is based on the

original dynamics model used to develop Mars Pathfinder, discussed in full by Cole and Waye (1993) with modifications for better correlation with the experimental results.

The model employs a time-stepping scheme, where at each time step the position of the supported mass is input for the change in airbag geometry. This is used to calculate the properties of the airbag operating medium (volume, pressure, and mass). At each time step, the condition for airbag venting is checked (limit pressure). If the condition is true, air flow through the venting orifice is modelled. These results are used as input for the next timestep.

1.2. Shape function

The shape of the cross-sectional area is a parameter that affects not only the stability of the airbag during the stroke but also its performance. In the mathematical model, a shape function describes the change of the cross-sectional area based on stroked distance. As Do (2011) discusses, the shape function assumes that the axial length of the cross section is constant during the stroke. It also neglects the elasticity of the airbag fabric, which, in fact, can greatly contribute to the performance of the airbag.

A semicylindrical shape was chosen. Shape function for volume of such a shape, shown in Figure 3, can be written as:

$$V(x) = \frac{\pi x}{4} (D + \pi(h - x))^2 + \frac{\pi^2 x^2}{2} \left(\frac{D}{2} + \pi(h - x) \right). \quad (2)$$

The first part of the Equation (2) describes the volume of a cylindrical part of the airbag. The second part describes the half of volume of the torus. Schematic of the semicylindrical shape stroking can be seen in the Figure 3.

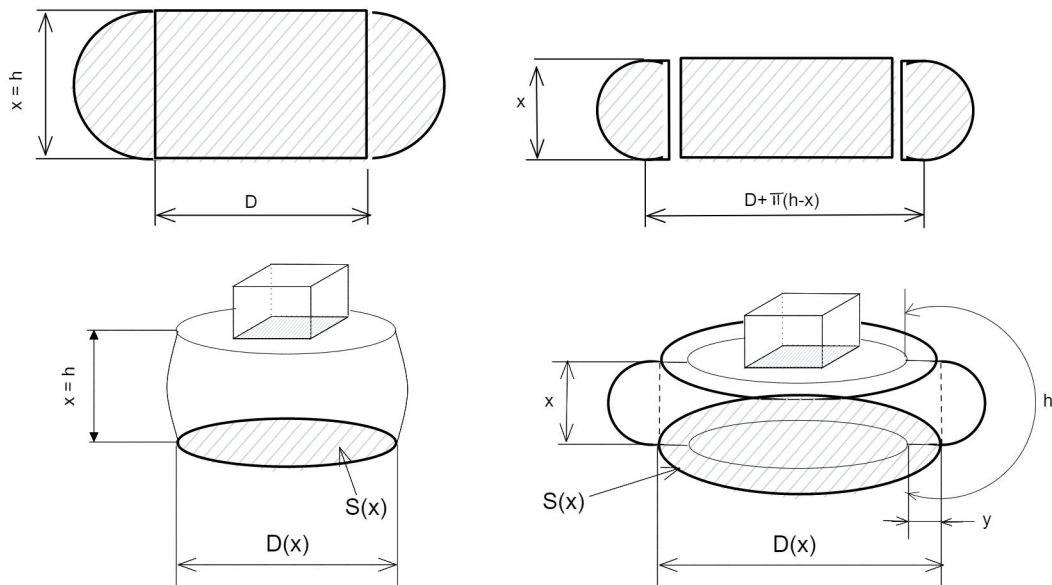


Figure 3. Un-stroked and stroked airbag shape function. Axial length is constant. Volume can be divided into two parts

1.3. Gas dynamics

When shape and therefore volume is known, gas dynamics can be investigated. The mathematical model assumes an airbag filled with atmospheric air behaving according to the ideal gas law and the isentropic nature of the process.

In each time step, the model calculates the change in pressure. It checks whether the conditions for the opening of the vent orifice are met. If not, the change in the decelerated mass velocity is calculated. If conditions are met, the model simulates an air flow through an orifice. It checks if the ratio of atmospheric pressure and pressure inside the airbag is greater than 0.582. Which is the critical pressure ratio for the ideal gas given by the Equation (3).

$$\frac{p_{atm}}{p_{abag}} = \left(\frac{\gamma + 1}{2} \right)^{\frac{\gamma}{1-\gamma}}. \quad (3)$$

If the pressure ratio is lower than critical, the flow through the orifice is subsonic. Flow in subsonic mode is governed by Equation (4). If the ratio is higher, the flow through the orifice is sonic and is governed by the Equation (5).

$$\frac{dm_p}{dt} = c_D S_{kr} p_{atm} \left(\frac{1}{RT_Z} \right)^{\frac{1}{2}} \left(\frac{2\gamma}{\gamma-1} \left(\frac{p_Z}{p_{atm}} \right)^{\frac{\gamma-1}{\gamma}} \right)^{\frac{1}{2}} \left(\left(\frac{p_{abag}}{p_{atm}} \right)^{\frac{\gamma-1}{\gamma}} - 1 \right)^{\frac{1}{2}}. \quad (4)$$

$$\frac{dm_p}{dt} = c_D S_{kr} p_Z \left(\frac{1}{RT_Z} \right)^{\frac{1}{2}} \left(\gamma \left(\frac{2}{\gamma+1} \right)^{\frac{\gamma+1}{\gamma-1}} \right)^{\frac{1}{2}} \left(\left(\frac{p_{abag}}{p_Z} \right)^{\frac{\gamma+1}{\gamma}} \right)^{\frac{1}{2}}. \quad (5)$$

1.4. Venting orifice

As shown by Lee et al. (1991), a properly designed venting orifice with fixed area improves the performance of airbags. An orifice with variable area can make an even greater contribution, as it brings the real deceleration stroke closer to the ideal one. In other words, it increases efficiency.

In the mathematical model, two distinct types of venting orifices are implemented. First, the fixed area orifice governed by an opening pressure parameter. When the opening pressure is reached, the orifice opens and allows air to flow into the atmosphere.

The second type is a variable area venting orifice. It is designed as an orifice closed by a lid. The lid is connected to one side with a hinge so that it can fully open or close the orifice. In the hinge, there is a torsional spring that reacts to the air pressure acting on the lid. By pretension and torsional stiffness of the spring it is possible to define the pressure of initial opening of the variable valve and the pressure of maximal opening of the valve. By using a burst membrane or cord ripping mechanism, a different opening and closing pressure can be set.

1.5. Discharge coefficient

Equations governing the flow of air through the orifice, both sonic and subsonic conditions, both depend upon the orifice discharge coefficient (c_D). This coefficient describes the energy loss of air flowing through the orifice caused mainly by friction and the viscous properties of air.

Values of discharge coefficient for thin-walled orifices were reported by Perry (1949), are widely accepted for airbag simulations. In Section 2.1 the modified value of discharge coefficient is shown for 20 mm thick wall. This modified c_D is better suited for the experimental model. Values reported by Perry are used for fixed area venting orifices when they are designed to be placed directly to the airbag wall.

1.6. Mathematical model validation

The first validation of the model was performed against previously published analytical airbag models with (Alizadeh et al., 2014; Lee et al., 1991; Rosato, 1999). This case investigates a rectangular airbag sized to 2.4x1.2x1.2 m equipped by a fixed, open orifice of an area of 0.129 m². The airbag supports a weight of 630 kg at impact velocity of 6.4 ms⁻¹.

The results of the current model compared to those of Alizadeh et al. (2014) are shown in the Figure 6b (Section 2.2).

1.7. Experimental validation of a mathematical model

An experimental model was designed and built to validate the mathematical framework against the experimental data and to account for various simplifications of the mathematical model. One of them, as Do (2011) mentions, omitting the airbag material elasticity is the most significant simplification. Since the mathematical model is currently set up for one 1 degree of freedom (DOF) the stability of chosen airbag shape is in question and shall be validated by experimental model.

The experimental model of an airbag was designed to be a semi-cylindrical shape with a diameter of 0.6 m and a height of 0.3 m. The airbag was made of MAKARO/L fabric and its seams were sealed for air tightness. A base plate with dimensions of 364x305 mm, made of 20 mm thick plywood, was placed on top of the airbag to support a mass of 10 kg. Experimental model during a test showed in Figure 4a. On the base plate, an orifice was made with an area of 0.0118 m². The orifice was equipped with a lid and sealed with rubber O-rings, showed in Figure 4b. The thickness of the O-rings then governs the pressure needed for the lid to open and allow the airbag to vent. The opening pressure was predetermined at 5500 Pa.

The airbag was then equipped with a triaxial accelerometer, internal pressure sensor and an open/closed lid state sensor. Sensors were connected to the data acquisition unit to store measured data at 5000 Hz.

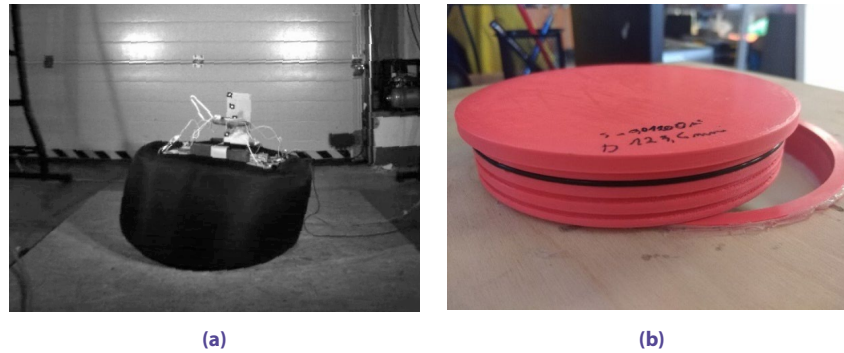


Figure 4. Experimental model. (a) – experimental model during a stroke. (b) – orifice lid equipped with one O-ring

A set of drop tests was performed. With each drop, the airbag was suspended at a predefined height, filled with pressurized air, for maximum volume and proper shape. The inside pressure equalized in a matter of 2 seconds to a level of atmospheric pressure. The drops were made at heights in the range of 0.45 to 2.95 m, with a step of 0.25 m. This corresponds to an impact velocity of 3–7.6 ms^{-1} . For each impact velocity a minimum of three measurements were made. The set contains 33 valid measurements. The results are discussed in the Section 2.4.

A smaller set of drop tests was conducted for the variable area vent. A valve described in 1.4 was 3D printed to fit the baseplate and to conserve the orifice area. The torque spring on a hinge was replaced with rubber bands that oppose the hinge. A potentiometer was added to the hinge for lid position sensing. The length, strength and pretension of the rubber bands were examined. The results are discussed in the Section 2.3.

1.8. Full-scale airbag design

With a mathematical model validated against the experimental results, a full-scale airbag could have been designed and its performance capabilities verified. Once performance was verified, the weight of the components could have been estimated for implementation assessment.

1.9. Airplane

For the implementation study, the ultralight airplane TL Stream was chosen. The Stream is in tandem, low-wing configuration with $m_{\text{TOW}} = 600$ kg and is equipped with a parachute recovery system of minimal activation height of 110 m AGL. The fact that the airplane has a low-wing configuration is favorable in terms of the area of contact of the airplane and the airbag.

1.10. Airbag design parameters

First, main design parameters for airbag design had to be set. First main parameter is allowed loading level of the crew members and second is speed of impact. The former was set to a level of 15 g 's, with duration no longer than 0.04 s, in the spine ward direction. According to Pesman

and Eiband (1956), this is the voluntary exposure level. Using a seatbelt and shoulder harness under these conditions did not cause injury. The latter parameter was set to 12 ms^{-1} , which is the impact speed of the free-falling airplane from a height of 10 m. This height is a 10% improvement of the minimal activation altitude for a given plane-parachute combination.

To attenuate such impact conditions, the system must be ready and fully inflated in 3 seconds.

1.11. Size, shape, and configuration

The initial height of the airbag was determined using the formula given by Knacke (1992) as:

$$-h = \frac{v_1^2}{2g(n\eta - 1)}. \quad (6)$$

With defined inputs and airbag efficiency 0.65, Equation (6) gives result 1.1 m.

Usable fuselage area determined by position of the engine bulkhead and rear pilot seat and across the inner wing, showed in Figure 5a. The total usable area of 3.7 m^2 corresponds to a circle of diameter of 2.6 m. This gives the smallest airbag in shape of a cylinder of 2.6 m diameter and 1.1 m height. Such a cylinder has a volume 4.45 m^3 .

Such a volume can hold 5.4 kg of air. By means of simple thermodynamic analysis devised by Do (2011), the total energy of the system can be determined to be 1187 kJ. To attenuate this energy, 4.02 kg of air must be vented from the airbag to the outside environment. That is 75% of the initial volume. This verified the attenuation capabilities of the designed airbag. Furthermore, it is likely that the final airbag will have a larger diameter for stability reasons.

Based on research of similar attenuation cases, it was determined to use a three-airbag system as a compromise to weight of the system, stroking stability, and complexity. One main airbag is placed under the crew seats and two smaller bags are placed under the inner wings for improved stability. Such a configuration, shown in Figure 5b, increased the total volume of air compared to the original estimate. It should also improve stability during the stroke due to the larger footprint area.

The full-scale airbag was designed with two types of vent orifices described in Section 1.4. The fixed area vent is

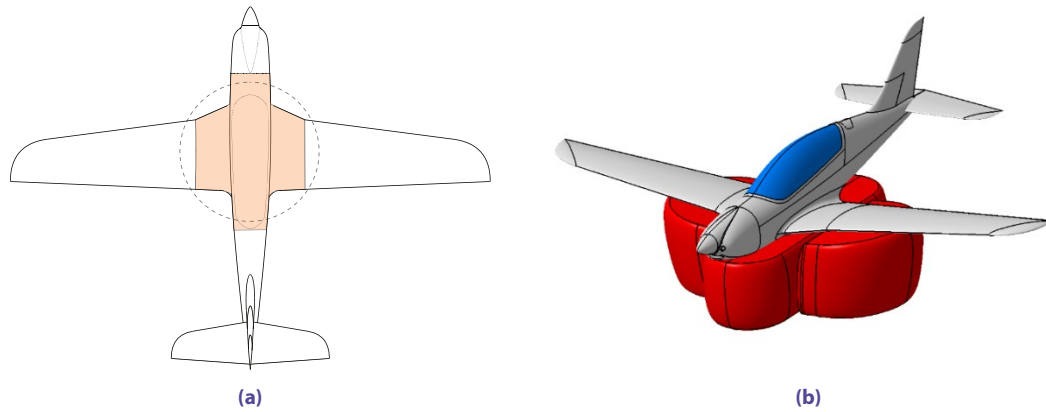


Figure 5. TL Stream. (a) – usable fuselage area; (b) – visualization of a system of three airbags

described by parameters: A_{fix} – the area of the fixed orifice, $p_{fix-open}$ – the pressure at which the fixed area orifice is opened. It is designed to be a burst-type orifice made in the airbag wall directly in the fabric. Once a critical pressure is reached, stitches of the lid of the orifice break and the orifice is then open for whole compression.

The variable area vent is described in detail in Section 1.4 and its parameters are characterized by: A_{Amax} – area of the orifice when lid is completely open, p_{A-open} – pressure of first opening, p_{A-max} – pressure at which lid is open to maximum, p_{A-min} – pressure at which the lid is completely closed.

1.12. Optimization of full-scale airbag parameters

With airbag parameters defined a brute force optimization method was implemented to find the optimal combination of parameters of the system of venting orifices. Aim of the optimization was to find the best performing combination parameters in terms of biggest amount of work done during the airbag compression within set limits as:

- $n_{max} < 15$ g – limiting parameter for crew health.
- $n_{min} > -1.5$ g – value greater than this indicates airbag rebound, which is undesirable.
- $s(t = end) < 0.1$ m – the height of the airbag at the end of the stroke cannot be higher than this for a full attenuation potential was used.
- $v_z(t = end) < -2$ ms⁻¹ – a value of the vertical speed of the decelerated mass at the end of the compression cannot be higher than this value to eliminate a possibility of a secondary impact.

A matrix of all possible combinations showed in the Table 1 resulted in 2592 possible solutions.

From all solutions only those that comply with rules set above were kept. Further reduction of viable solutions was achieved by eliminating the results with oscillating behavior in the vent with variable area. This behavior is caused by a slow pressure decrease while the airbag is still stroking. Closing the variable area vent causes an increase

Table 1. Matrix of optimized intervals and its values

Parameter	Lower range	Upper range	Num of points
p_{A-open} [Pa]	3000	12000	6
p_{A-max} [Pa]	1000	1000	1
p_{A-min} [Pa]	3000	12000	6
$p_{fix-open}$ [Pa]	2000	8000	6
A_{Amax} [m ²]	0.3	1.9	6
A_{fix} [m ²]	0.15	0.7	2

in pressure that causes repeated opening of the vent. This resulted in 32 sets of parameters with valid results.

The results of the parameter optimization are given in Section 2.4.

1.13. Airbag implementation

Once volume of inflated airbag shape is known, a total surface area can be determined. From the surface area, a volume of packed airbag can be devised. The total volume was determined to be 10.23 m³, the surface area of the three airbags in the system was determined to be 37.55 m².

Using MAKARO / L fabric, with thickness of 0.82 mm, the volume of the fabric is 0.031 m³. If 10% of the volume is added to account for folds and sewing, the volume of the packed airbag is 0.034 m³. The mass of fabric of such an area is less than 2.7 kg.

Two types of attachment to the aircraft frame were developed. Simpler form, a cylinder attached under the fuselage between the legs of the landing gear. For example, a cylinder with diameter of 0.25 m and length of 0.7 m is sufficient to accommodate a given volume.

More complicated form of custom-made cover for bottom part of the fuselage. If the allowable area in the bottom part of a fuselage is used to be 1.6 m², the thickness of 20 mm is needed to accommodate the given volume.

Both solutions are described to give a better idea of the size of the design. For further work, both need to be developed in more detail.

1.14. Airbag inflation sizing

To accommodate a condition set up at the beginning of the section, to inflate the airbag under 3 s, a filling method was proposed. In comparison to the traditional automobile industry, the filling time is longer in order of magnitude and can take advantage of simpler solutions. This study suggests using an EDF, where only four components are needed: EDF, power source, power management and control unit.

The size of the EDF is limited by the market offer. The largest commercial EDF, by JP Hobby Europe (n.d.), has an inner diameter of 120 mm and weighs 0.7 kg. From Froude’s theory of an ideal propulsor, the speed of the flow at the propulsor plane can be estimated as:

$$P = T v \rightarrow v = \frac{P}{T}. \tag{7}$$

With known power of 9631 W and thrust of 108 N, provided by manufacturer, the theoretical mass flow of air through the EDF can be estimated as

$$\dot{m}_T = \rho S v = \rho S \frac{P}{T}. \tag{8}$$

And gives theoretical mass flow through EDF 1.1 kgs⁻¹. The Equation (8) for mass flow can be rewritten, to obtain time needed for filling the airbag volume:

$$t = \frac{\rho V}{k \dot{m}_T}. \tag{9}$$

To fill the volume of the main airbag (Equation (9)), while using 2x120 mm EDF in theory 1.5 seconds is needed. To fill one of the side bags with one EDF unit, 3 seconds are needed. In total, 4 EDF units should be able to fill all volumes in less than 3 seconds.

The power source for an EDF needs to be able to output 72–78 V and 150 A. To run for at least 60 seconds, a capacity of 2500 mAh is needed. One cell of a Li-pol battery with the capacity needed, on average weights 60 grams. Therefore, a pack of 18 cells weighs less than 1.1 kg.

The speed controller is critical component. The one recommended by the EDF manufacturer is capable of handling 200 A and weighs 0.15 kg.

All weight important parts needed to power one EDF unit for 60 seconds weighs 1.95 kg. Therefore, the system of four EDF and its components weighs 7.8 kg.

1.15. System activation

The proposed system is intended to work with a rescue parachute. Activation of airbag inflation can be combined with activation of the rescue parachute, which is done by pulling the activation handle in a cabin by one of the crew members. This solution eliminates complex devices for the evaluation of crash situations, but it requires timely human input.

2. Results

In this section the results of previous sections are discussed.

2.1. Modification of the discharge coefficient

During development, it was noted that the discharge coefficients (c_D) used in the mathematical model are valid for thin-walled orifices (Perry, 1949). A simple CFD simulation was conducted for a 20 mm thick wall and pressure ratio in the range of 0.91–0.98 where most of the experiments were done. The difference in c_D can be seen in the Figure 6a. The curve shown can be approximated by a polynomial:

$$c_D = 27.87888 \left(\frac{p_{kr}}{p_u} \right)^3 - 79.69357 \left(\frac{p_{kr}}{p_u} \right)^2 + 75.60716 \left(\frac{p_{kr}}{p_u} \right) - 23.18063. \tag{10}$$

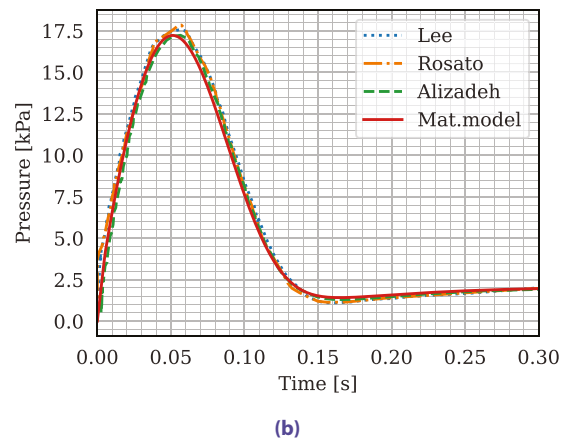
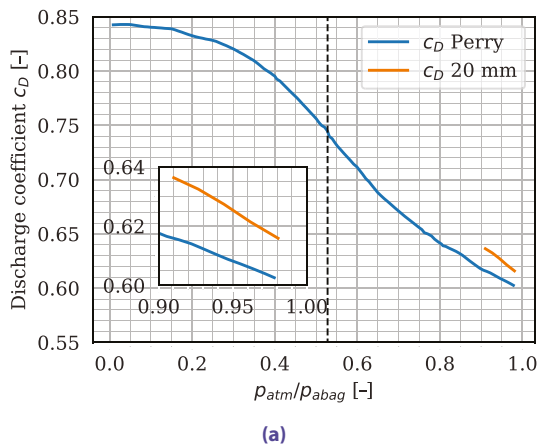


Figure 6. Mathematical model. (a) – comparison of c_D devised for thin-walled orifices and for 20 mm thick wall; (b) – mathematical model validation against published results (Alizadeh et al., 2014; Lee et al., 1991; Rosato, 1999)

2.2. Validation of the mathematical model

Validation of the described mathematical model is shown in Figure 6b. The shape of the pressure response of the model appears to be the same as in the mentioned models. In magnitude, there is a slight difference no greater than 0.1 kPa, less than 0.5% of difference. The model can be considered valid.

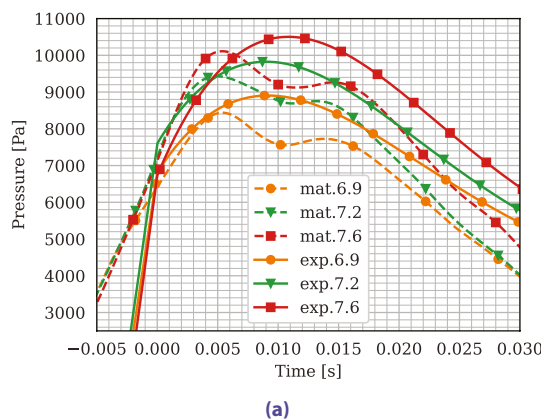
2.3. Comparison of the mathematical and the experimental models

Figure 7a shows a comparison of the pressure response of both the mathematical and experimental models for the same impact conditions in the first set of drop tests. The figure shows that the mathematical model delivers satisfactory results in the range of impact velocities between 6.9–7.6 ms^{-1} . The differences in predicted and measured pressure are lower than 5%. Higher speeds have not been verified due to physical limitations of the testing lab. The mathematical model should be corrected for lower impact velocities. Nonetheless, future interest lies in higher impact velocities.

Figure 7b shows a comparison of the effect of the variable area vent on the pressure and acceleration response obtained in the second set of drop tests. The fixed area and the variable area orifices are compared for the impact velocity of 4.85 ms^{-1} . The maximum acceleration values have been reduced from 12.5 g to 7 g. That is a significant reduction of 44%. For such a significant reduction at other impact velocities, the right torsional stiffness has to be found experimentally.

2.4. Results of parameter optimization

Venting orifice parameters optimization described in the Section 1.12 resulted in 32 valid sets, from which four combinations of parameters were chosen. Each set of parameters is called by its identification number. Parameter values are in the Table 2. The Figure 8 shows displacement, velocity, G force of decelerated mass and pressure response of the airbag for the cases listed in the Table 2.



(a)

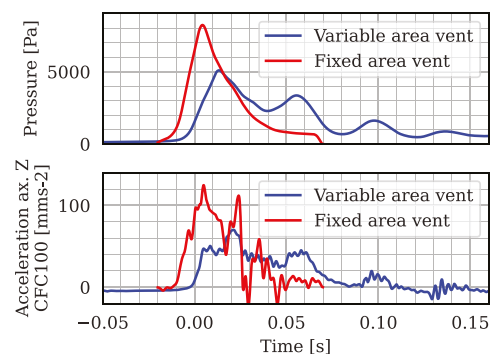
Table 2. Results of the parameter optimization

ID:	2524	2104	2581	2509
$p_{A\text{-open}}$ [Pa]	12000	10200	12000	12000
$p_{A\text{-max}}$ [Pa]	12000	12000	12000	10200
$p_{A\text{-min}}$ [Pa]	2000	3200	8000	8000
$A_{A\text{max}}$ [m^2]	0.94	0.94	0.30	0.30
A_{fix} [m^2]	0.15	0.15	0.70	0.70
$p_{\text{fix-open}}$ [Pa]	1000	1000	1000	1000
s (end) [m]	0.06	0.09	0.00	0.00
v (end)[ms^{-1}]	-0.41	-0.41	-1.98	-1.99
n_{max} [-]	12.99	11.77	14.29	13.86
p_{max} [Pa]	13093	12678	13703	13319
W [J]	49312	49103	48505	48493

The first set, ID 2542, resulted in the largest amount of work done by the airbag. The second set, ID 2104, has the biggest $W/W_{T_{\text{MAX}}}$. It is the ratio between the work carried out by the airbag and the maximal theoretical work carried out by the ideal absorber with constant 15 g's deceleration.

Cases with ID 2509 and 2581 are chosen, because they meet all the conditions listed in the Section 1.12, but opposed to the first two have small area of variable area vent and big area of fixed area vent. This could mean a simpler implementation to the airframe. It is worth noting that the work done by the last two solutions is the lowest of all remaining solutions. The difference is only 1000 J, less than 2% of the work done by the first solution.

The difference in compression time is also a parameter worth mentioning. We can see that the solutions 2542 and 2104, due to the smaller values of the maximum acceleration, have a more gradual velocity profile and thus takes longer to travel the distance to full compression. Opposed to the solutions 2581 and 2509, which have higher acceleration values, steeper velocity profile and shorter compression time. Although this difference is on the order of one tenth of a second it may affect the resulting stability of the system, where longer time means a higher risk of



(b)

Figure 7. Results. (a) – comparison of mathematical and experimental model pressure responses; (b) – comparison of variable and fixed area ven for impact speed of -4.85 ms^{-1}

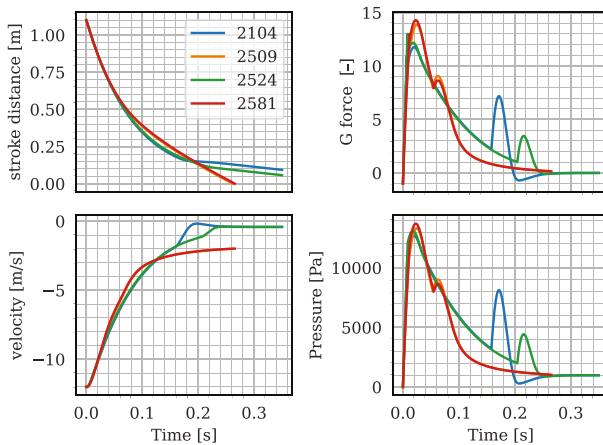


Figure 8. Displacement, velocity, G force of decelerated mass and pressure response of the airbag for the chosen sets of parameters, listed in Table 2

unstable behavior. This, however, contradicts one of the main principles of shock absorption – whereby increasing the time or path of the impact force will reduce the maximum load.

3. Discussion

On the TL Stream, a preliminary design for the whole-body, under-fuselage rescue airbag that will support the parachute recovery system was completed. Beginning design limitations included an impact speed of 15 ms⁻¹ and a limit load of 15 g's.

The initial sizing was confirmed using a mathematical model that had undergone experimental validation. The venting orifices' parameters were optimized in order to achieve maximum performance. Four of the 32 valid results from the optimization were looked at in more detail. The improvement in performance might be brought on by a more sophisticated optimization technique. But it is anticipated to be in the order of percent.

The presented optimization results seem to point to the 2509 solution. As it has a small variable area vent out of 4 selected solutions which means easier implementation. It has faster stroking time, which is favourable for system stability. And it has smaller G-force load values, which is favourable for crew health.

The identical set of characteristics specified in Section 2.4, presented in Table 2, were simulated with the parachute recovery system's usual impact speed to verify system behaviour with the parachute fully inflated.

All four proposed parameter sets perform within the limits specified in Section 1.12. It demonstrated that the system can operate within predefined parameters and can reduce the minimum height of activation by 10%. In the event of an activation altitude greater than the minimum, the system will continue to function to safeguard the crew.

The largest weight penalty comes from the EDF's power source, as stated in Section 1.14. The system consists of four EDFs and a power source weighing 7.8 kg. The airbag

material's mass was determined to be 2.7 kg. The mass of the required coverings and related installation equipment was determined to be no more than 5 kg. The entire mass of the system was established to be no more than 15 kg. This raises the rescue system's weight ratio to the maximum takeoff weight from 2% to 4.7%. According to Knacke (1992), the usual rescue system weight to maximum take-off weight ratio can be as high as 10%.

The authors are aware of simplifications done during the process of implementation assessment. The goal of this work was to determine whether such an application for airbags is viable in terms of weight penalty and airbag performance.

The purpose of this research was to see if such an application for airbags is feasible in terms of weight penalty and airbag performance. The authors are aware of simplifications made throughout the implementation evaluation process and are confident in 15 kg weight of the system.

Conclusions and future work

The study of the viability assessment of the new type of crew protection in the small airplane category has been presented in the paper. In order to evaluate new, unparallel means of protection in UL planes the by the underfuselage airbag, a multidisciplinary approach was used. Approach is encompassing full-size airbag design and sizing, experimental methodology for its verification, and mathematical model of airbag performance. The device created by the research that has been presented can reduce the PRS's minimal activation altitude by 10%. The rescue system's weight ratio to the allowed takeoff weight rises from 2% to 4.7%. Future research should concentrate on examining the airbags stability in forward motion caused by wind. The underfuselage airbag is regarded as a feasible option for improving crew safety on small aircrafts.

Funding

This work was supported by the Technologická agentura České Republiky under Grant number TH02010204.

Author contributions

TH contributed the central idea, performed the design work, experiments, optimization work, and analysed most of the data. He wrote the paper and was responsible for submission process.

RG was responsible for creating the biggest part of mathematical model, done CFD simulation and helped with experiments.

RP contributed to refining the ideas.

Disclosure statement

Authors declare that they do not have any competing financial, professional, or personal interests from other parties.

References

- Alizadeh, M., Sedaghat, A., & Kargar, E. (2014). Shape and orifice optimization of airbag systems for UAV parachute landing. *International Journal of Aeronautical & Space Sciences*, 15(3), 112–121. <https://doi.org/10.5139/IJASS.2014.15.3.335>
- Astronautix. (2023). Luna. <http://www.astronautix.com/l/luna.html>
- Botton, D. (2021). F-111 rescue system. <https://doi.org/10.1515/9781644699096-012>
- Browning, A. C. (1963). *A theoretical approach to air bag shock absorber design* by A.C. Browning. Royal Aircraft Establishment.
- Cole, J., & Waye, D. (1993). BAG: A code for predicting the performance of a gas bag impact attenuation system for the PATHFINDER lander. *Osti*. <https://doi.org/10.2172/10106335>
- Defense Update. (2005, December 15). Rotorcraft External Airbag Protection System (REAPS). *Defense Update*. https://defense-update.com/20051215_reaps.html
- Do, S. (2011). *An airbag-based crew Impact attenuation system for the Orion crew exploration vehicle*. MIT Libraries.
- Elbit Systems. (2023). *Skylark™ I – LEX*. Elbit Systems. <http://elbitsystems.com/products/uas/skylark-i-lex/>
- Hurley, T. R. (2002). *Small airplane crashworthiness design guide* [Design Guide]. Simula Technologies.
- JP Hobby Europe. (n.d.). EDF Ducted Fan JP Hobby 120mm + motor 18s 510Kv (CW). JP HOBBY Europe. Retrieved September 11, 2022, from <https://www.jphobby.eu/en/jp-hobby/2289-edf-ducted-fan-jp-hobby-120mm-motor-18s-510kv-cw.html>
- Knacke, T. W. (1992). *Parachute recovery systems: Design manual* (1st ed.). Para Pub.
- Lee, C., Rosato, N., & Lai, F. (1991, April 9). An investigation of improved airbag performance by vent control and gas injection. In *11th Aerodynamic Decelerator Systems Technology Conference*. San Diego, CA, U.S.A. <https://doi.org/10.2514/6.1991-892>
- Londonson, D. (2017). SOARS for GA and experimental aircraft. AMSAFE. <https://www.amsafe.com/airbag-systems/soars/>
- Manta Air. (2023). *UAV and Drone Parachute Recovery*. Manta Air. https://manta-air.com/uav_safety_and_recovery_systems/
- Norman, L. C., & Kiker, J. W. (1967). *Spacecraft landing systems* (SAE Technical Paper No. 670403). SAE International. <https://doi.org/10.4271/670403>
- National Transportation Safety Board. (2011). *Review of US civil aviation accidents calendar year 2011* (Safety Study NTSB/SS-11/01). NTSB.
- Perry, J. A. (1949). Critical flow through sharp-edged orifices. *Transactions of the American Society of Mechanical Engineers*, 71(7), 757–764. <https://doi.org/10.1115/1.4017216>
- Pesman, G. J., & Eiband, A. M. (1956, November). *Crash Injury* (Report NACA-TN-3775). UNT Digital Library. <https://digital.library.unt.edu/ark:/67531/metadc55999/>
- Rosato, N. P. (1999). *Passive airbag vent control valve study* (Technical Report NATICK/TR-00/010). U.S. Army Solider an Biological Chemical Command Solider System Center.
- Stein, J., Sandy, C., Wilson, D., Sharpe, G., & Knoll, C. (2003, April 7). Recent developments in inflatable airbag impact attenuation systems for Mars exploration. In *44th AIAA/ASME/ASCE/AHS/ASC Structures, Structural Dynamics, and Materials Conference*. Norfolk, Virginia. <https://doi.org/10.2514/6.2003-1900>
- Šorf, O. (2015). *Padákové záchranné systémy lehkých sportovních letadel* [Vysoké učení technické v Brně. Fakulta strojního inženýrství]. <http://hdl.handle.net/11012/38094>
- Tutt, B., Gill, S., Wilson, A., & Johnson, K. (2009, May 4). A summary of the development of a nominal land landing airbag impact attenuation system for the Orion Crew module. In *20th AIAA Aerodynamic Decelerator Systems Technology Conference*. Washington. <https://doi.org/10.2514/6.2009-2922>

Notations

Abbreviations

- AGL – Above Ground Level;
 DOF – Degree of Freedom;
 EDF – Electric Ducted Fan;
 PRS – Parachute Recovery System;
 REAPS – Rotorcraft External Airbag Protection System;
 VTOL – Vertical Take Off and Landing.

Variables and functions

- A_{Amax} – area of the orifice with variable area when lid is completely open;
 A_{fix} – area of an orifice with fixed area;
 c_D – discharge coefficient;
 D – diameter of an airbag;
 D_0 – nominal diameter of a parachute;
 g – gravitational acceleration;
 h – height of an airbag;
 k – is the number of EDF units;
 m_p – air mass;
 \dot{m}_T – air mass flow;
 m_{TOW} – maximal take-off mass;
 n – allowable load;
 n_{pc} – parachute constant for filling time;
 P – power consumption of a propulsor;
 P_{abag} – pressure inside of an airbag;
 P_{A-max} – pressure at which the lid of a variable area orifice is open to maximum (at A_{Amax});
 P_{A-min} – pressure at which the lid of a variable area orifice is completely closed;
 P_{A-open} – pressure at which the orifice with variable area opens;
 P_{atm} – atmospheric pressure;
 $P_{fix-open}$ – pressure at which the orifice with fixed area opens;
 P_{kr} – pressure at critical plane – the orifice throat;
 P_u – pressure upstream of the orifice e.g., inside of the airbag;
 R – specific gas constant;
 S_{kr} – orifice area at critical plane;
 T – air temperature;
 T – thrust of a propulsor;
 t_f – time to fill the parachute;
 V – volume of an airbag;
 v_1 – system impact speed;
 v_{ls} – velocity at the line stretch;
 W – work done by an airbag;
 γ – Poisson constant;
 γ – ratio of specific heat;
 η – efficiency;
 ρ – air density.